

Quantum Embedding for Correlated Electronic Structure in Large Systems and the Condensed Phase (Princeton University): ER46960-SC0010530

- PI: Garnet Kin-Lic Chan
- Final technical report: 9/1/15-8/31/16

I. RESEARCH ACCOMPLISHMENTS

Publications with full or partial support from this grant.

1. “Ab initio determination of the crystalline benzene lattice energy to sub-kilojoule/mole accuracy” J. Yang, W. Hu, D. Usvyat, D. Matthews, M. Schuetz, G. K.-L. Chan, *Science*, 345, 640 (2014)
2. “Exact and optimal quantum mechanics/molecular mechanics boundaries”, Q. Sun and G. K.-L. Chan, *J. Chem. Theory Comput.*, 10, 3784 (2014)
3. “Intermediate and spin-liquid phase of the half-filled honeycomb Hubbard model” Q. Chen, G. H. Booth, S. Sharma, G. Knizia, G. K.-L. Chan *Phys. Rev. B*, 89, 165134 (2014)
4. “Solutions of the two-dimensional Hubbard model: Benchmarks and results from a wide range of numerical algorithms”, J. P. F. LeBlanc et al, *Phys. Rev. X*, 5, 041041 (2015)
5. “A transformed framework for dynamic correlation in multireference problems”, A. Y. Sokolov, G. K.-L. Chan, *J. Chem. Phys.*, 142, 124107 (2015)
6. “Advances in molecular quantum chemistry contained in the Q-Chem 4 program package”, Y. Shao et al, *Mol. Phys.* 113, 184 (2015)
7. “Spectral functions of strongly correlated extended systems via an exact quantum embedding”, G. H. Booth, G. K.-L. Chan, *Phys. Rev. B* 91, 155107 (2015)
8. “From plane waves to local Gaussians for the simulation of correlated periodic systems” G. H. Booth, T. Tsatsoulis, G. K. Chan, A. Grueneis, *J. Chem. Phys.*, 145, 084111 (2016)
9. “Five years of density matrix embedding theory”, S. Wouters, C. A. Jimenez-Hoyos, G. K.-L. Chan, *arXiv:1605.05547* (2016)
10. “Cluster size convergence of the density matrix embedding theory and its dynamical cluster formulation: a study with an auxiliary-field quantum Monte Carlo solver”, B.-X. Zheng, J. S Kretchmer, H. Shi, S. Zhang, G. K.-L. Chan, *Phys. Rev. B*, 045103 (2017)
11. “Correct quantum chemistry in a minimal basis from effective Hamiltonians”, T. J. Watson Jr, G. K.-L. Chan, *J. Chem. Theory and Comput.*, 12, 512 (2016)
12. “Density matrix embedding theory for interacting electron-phonon systems”, B. Sandhoefer, G. K.-L. Chan, *Phys. Rev. B*, 94, 085115 (2016)
13. “Ground-state phase diagram of the square lattice Hubbard model from density matrix embedding theory”, B. X. Zheng, G. K.-L. Chan, *Phys. Rev. B*, 93, 035126 (2016)
14. “A Practical Guide to Density Matrix Embedding Theory in Quantum Chemistry”, S. Wouters, C. A. Jimenez-Hoyos, Q. Sun, and G. K.-L. Chan *J. Chem. Theory Comput.*, 12, 2706 (2016)
15. “Spectral Functions of the Uniform Electron Gas via Coupled-Cluster Theory and Comparison to the *GW* and Related Approximations”, J. McClain, J. Lischner, T. Watson, D. A Matthews, E. Ronca, S. G Louie, T. C. Berkelbach, G. K.-L. Chan, *Phys. Rev. B*, 93, 235139 (2016)
16. “A time-dependent formulation of multi-reference perturbation theory”, A. Y. Sokolov, G. K.-L. Chan, *J. Chem. Phys.*, 144, 064102 (2016)

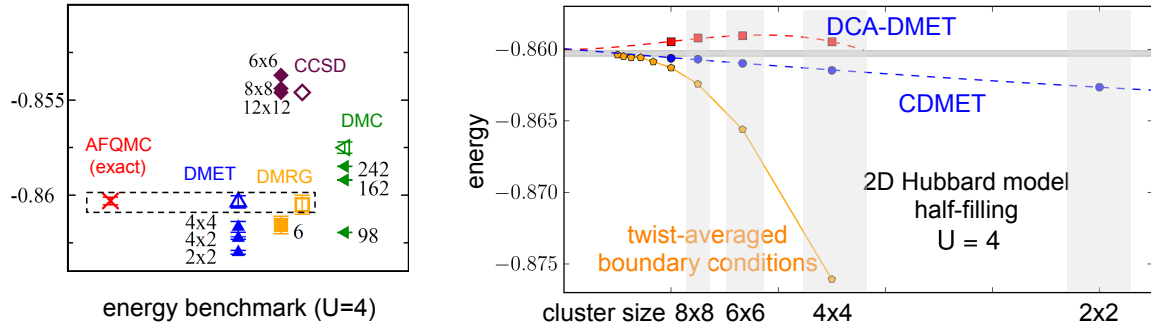


FIG. 1: Left: DMET benchmark energies (half-filling $U = 4$) agree well with the best state-of-the-art data from AFQMC and DMRG (Simons Collaboration [1]). Right: Cluster size convergence of DMET (cellular and DCA formulations): embedded cluster energies converge to the TDL *much* faster than when using twist-averaged boundary conditions [2].

17. “N-Electron Valence State Perturbation Theory Based on a Density Matrix Renormalization Group Reference Function, with Applications to the Chromium Dimer and a Trimer Model of Poly (p-Phenylenevinylene)”, S. G., M. A. Watson, W. Hu, Q. Sun, G. K.-L. Chan, *J. Chem. Theory Comput.*, 12, 1583 (2016)
18. “Matrix Product Operators, Matrix Product States, and ab initio Density Matrix Renormalization Group algorithms”, G. K.-L. Chan, A. Keselman, N. Nakatani, Z. Li and S. R. White, *J. Chem. Phys.*, 145, 014102 (2016)

We briefly describe some selected results below. (In this section, “Pub.” refers to numbers above).

1. *Developments in density matrix embedding.* DMET is a quantum embedding theory that we introduced at the beginning of the last funding period, around 2012-2013. Since the first DMET papers, which demonstrated proof-of-principle calculations on the Hubbard model and hydrogen rings, we have carried out a number of different developments, including:

- Extending the DMET technology to compute broken symmetry phases, including magnetic phases and superconductivity (Pub. 13).
- Calibrating the accuracy of DMET and its cluster size convergence against other methods, and formulation of a dynamical cluster analog (Pubs. 4, 10) (see Fig. 1).
- Implementing DMET for ab-initio molecular calculations, and exploring different self-consistency criteria (Pubs. 9, 14).
- Using embedding to define quantum classical interfaces Pub. 2.
- Formulating DMET for spectral functions (Pub. 7) (see Fig. 1).
- Extending DMET to coupled fermion-boson problems (Pub. 12).

Together with these embedding developments, we have also implemented a wide variety of impurity solvers within our DMET framework, including DMRG (Pub. 3), AFQMC (Pub. 10), and coupled cluster theory (CC) (Pub. 9).

It is also worth noting that in the last few years, many other groups have started to contribute to different aspects of DMET [3-6].

2. *Applications to correlated lattice models.* We have applied DMET in many different settings ranging from molecules (Pub. 9), to surfaces, to different kinds of correlated lattice models (Pubs. 3, 4, 7, 10, 12, 13). Through the economy of the DMET formulation, together with efficient ground-state solvers, we have used larger impurity clusters than previously employed in zero temperature studies, e.g. up to 100 sites, (Pub. 10).

Amongst these applications, we have carried out several studies on the 1-band Hubbard model on a square lattice, the prototypical model for the high T_c cuprates (Pub. 13). Here we have computed a highly-converged ground-state phase diagram, a long-standing goal of numerical simulation (Fig. 2). Our worst case estimated error, across the range of parameters, is between 0.001-0.01t (about 3-30K in physical units). While this accuracy has been achieved before for select values of the Hubbard U and doping parameters, this is, to our knowledge, the first full phase diagram computed at this level of precision. An independent confirmation of the accuracy of our results has recently been

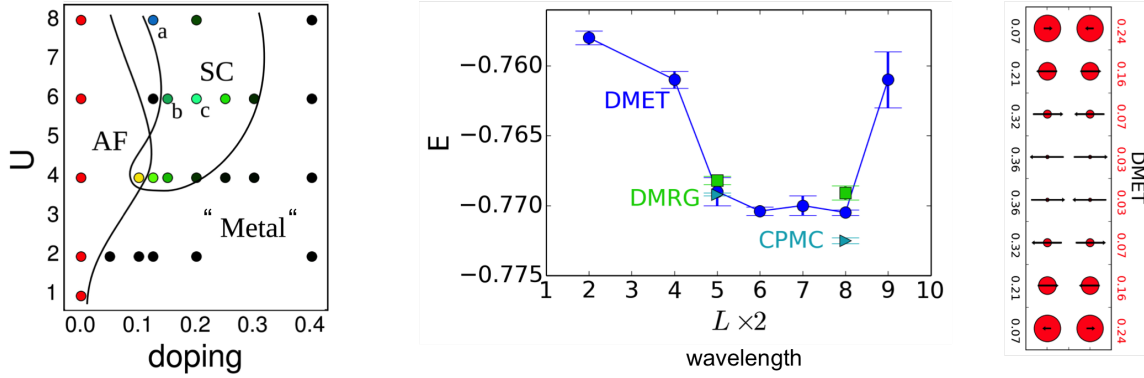


FIG. 2: Left: DMET ground-state phase diagram of the Hubbard model, showing AFM and SC regions. The “metallic” region denotes a region where order is too weak to detect numerically [7]. Right: Stripes in the underdoped region: energy vs. wavelength for 3 methods, showing the remarkable near-degeneracy of stripes of wavelengths between 5 and 8.

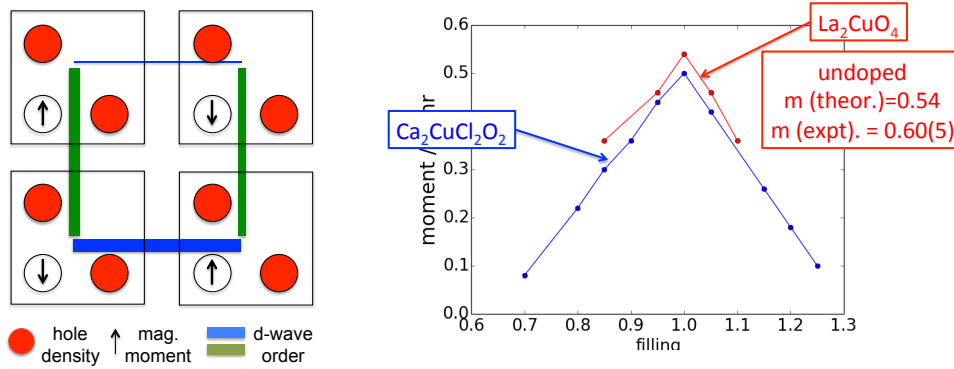


FIG. 3: Left: Magnetic, charge, and pairing order in the 3-band model (2x2 unit cell) at 1/8 doping, showing inhomogeneous pairing order within the 2x2 cell. Right: Preliminary ab-initio DMET calculation for magnetic order as a function of doping in La_2CuO_4 and $\text{Ca}_2\text{CuCl}_2\text{O}_2$. These show the correct material trends and even absolute magnitudes.

provided by the Simons survey, which examined the performance of 9 numerical methods, including DMET, at a few points in the Hubbard phase diagram (Pub. 4). Our DMET calculations provide new ground-state information beyond what has been seen in DCA simulations, as in such studies even the lowest temperatures accessed do not reach the energy scale of competing ground-state phases. One important conclusion is that we find strong evidence for robust ground-state superconductivity as well as for coexisting competing magnetic orders, including several kinds of inhomogeneous orders in the underdoped region.

Recently, in a multi-method collaboration with Corboz, Noack, White, and Zhang, we have carried a further, more detailed, DMET study of the underdoped region, to definitively resolve the order. In conjunction with several methods, we establish that the lowest energy order at 1/8 doping is a vertically striped state (see Fig. 2), with a charge wavelength of 8 and vanishing superconducting order. Intriguingly, our DMET calculations find almost perfect degeneracy between stripes of wavelengths 5-8, on the scale of 0.001t per site, and this remarkable degeneracy is supported also by the other numerical methods. This study, currently under revision for Science (arxiv:1701.00054), highlights a new fluctuation mode that clearly will be important in the physics of the underdoped region. To our knowledge, this may be the first conclusive numerical resolution of competing order in the underdoped region of the 2D Hubbard model.

Although the precise control that DMET now provides for the ground-state of the 2D Hubbard model is gratifying, it is important to remember that the model is artificial. Real cuprate materials contain many more Hamiltonian terms: long-range Coulomb, multi-orbital interactions, and disorder, all of which likely break the degeneracies observed in the Hubbard model. For the physics of real materials, it seems urgent to include these additional effects. We have been working hard to set up the infrastructure for ab-initio embedded calculations, and preliminary results in this

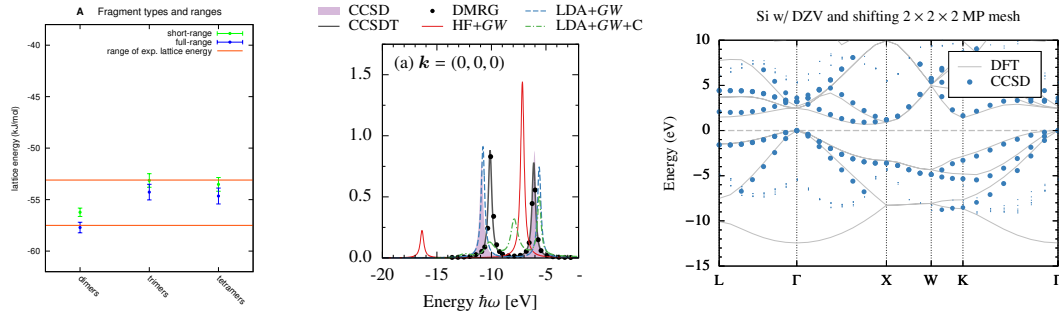


FIG. 4: Left. Convergence of different many-body coupled cluster contributions in the benzene crystal lattice energy [8]. Middle. Spectral function of the 3D UEG at $r_s = 4$, showing the good agreement between CCSDT and benchmark DMRG results [9]. Right. Correlated density of states of Si from a preliminary EOM-CCSD implementation.

direction, for the 3-band cuprate Hubbard model and for an ab-initio 40 band cuprate representation are shown in Fig. 3.

3. *Coupled cluster calculations in the condensed phase.* We have also explored using coupled cluster methods in the condensed phase, building off our earlier work on local molecular coupled cluster methods, funded in earlier rounds by the DOE. To investigate the potential of condensed phase coupled cluster calculations, we carried out a simple initial exercise, namely to compute as accurately as possible the lattice energy of the benzene molecular crystal, a well-studied benchmark for crystal structure total energy methods (Pub. 1). We aimed to establish whether or not we could achieve the same absolute predictive accuracy that coupled cluster provides in molecular problems. Because the molecular crystal lattice energy can be obtained from a series of supramolecular calculations via the many-body expansion, we could simply reuse our existing local coupled cluster molecular codes. With large basis sets and high levels of correlation, we found that we could determine the lattice energy to within an estimated uncertainty of about 0.75 kJ/mol, similar to the accuracy achievable in molecular thermochemistry.

Highly accurate lattice energies are essential to distinguish between the stability of crystal polymorphs. Our calculation was the first to achieve an accuracy below the 1 kJ/mol polymorph energy scale. Interestingly, we found that our lattice energy estimate was significantly different from the experimental estimates (by about 2-3 kJ/mol). Since our estimate was obtained by converging the solution of the Schroedinger equation without further approximations, such a deviation could only come from errors in the experimental estimate! As we showed in our analysis in Pub. 1, this was indeed the case, as the experimental number employed an incorrect thermal extrapolation and zero point energy correction. Even though these systematic calculations are relatively expensive, the ability to compute lattice energies to this accuracy has important implications for crystal structure prediction, as today most search algorithms can identify a set of plausible correct polymorph structures, and but lack the ability to correctly rank the few candidates in energy.

While our calculation on the benzene crystal targeted the ground-state, the simulation of materials spectra is a more central objective. To study the use of coupled cluster theory for condensed phase spectra, we first considered the simplified setting of the 3D uniform electron gas (Pub. 15). Here, we computed single-particle spectral functions using equation-of-motion coupled cluster and compared them against the GW and GW+C (cumulant) approximations, as well as DMRG benchmarks. We found that the CC spectral functions significantly improved on GW and GW+C, particularly in the satellite regions (Fig. 4). Further, the CC spectra had no dependence on the initial mean-field state, unlike standard single-shot GW.

The success of the above exercises provides real motivation to develop and explore genuine periodic implementations of ground-state and spectral coupled cluster methods, for condensed phase energetics and spectra beyond existing ab-initio diagrammatic approximations. This is one of the major thrusts of our current work.

4. *Model Hamiltonian derivation.* We have continued to work on methods to derive model Hamiltonians from ab-initio calculations, in particular through numerical canonical transformations. The most common difficulty is the divergence of canonical transformations near perturbation theory singularities. We found a particularly simple regularization of perturbation theory that allows for qualitatively accurate model Hamiltonians in molecules to be derived by a simple second order canonical transformation (Pub. 11).

5. *Multi-reference perturbation theory solvers.* For realistic impurity models associated with bare Hamiltonian interactions, as of interest in the current proposal, one has to treat a wide range of energy scales that includes a set of strongly correlated degrees of freedom coupled to a larger number of weakly correlated, higher energy orbitals. We

have been investigating multi-reference perturbation theory methods, and in particular density matrix renormalization group plus perturbation theory, as a practical approach to this problem (Pubs. 5, 16, 17). We have extensively tested our DMRG + PT solvers in strongly correlated molecular applications (see e.g. Fig. 4 where we show one of the most accurate binding curves for the Cr₂ molecule, the archetype of a strongly correlated molecule, determined using DMRG + SC-NEVPT2).

6. *Gaussian basis software infrastructure for periodic many-body methods.* Behind any ab-initio many-body calculation lies many layers of computational infrastructure. In molecular quantum chemistry, these various layers - integral transformations, Hartree-Fock solvers, Gaussian integrals, basis sets - are well decoupled, and in a structured molecular code one can choose to work on the different components (e.g. on correlation methods) without concerns about the other layers (such as basis sets). However, the same infrastructure and separation of components is less well-developed in ab-initio periodic codes. One reason is the historical emphasis on DFT, where the supporting technology (e.g. for many-body matrix elements) has not been needed, while another factor is the use of plane-wave basis sets, which due to their large number, prevent the straightforward construction and storage of many-body wavefunctions and matrix elements, thus complicating the separation of responsibilities.

In the last funding period, we have been building a new open-source simulation package, PySCF (github.com/sunqm/pyscf) to simplify the development of electronic structure methods, and many-body quantum methods in particular. Our code is unusual in that it aims to achieve equal capabilities for the quantum chemical treatment of molecules, and for many-body simulations of materials. Our technology is based on Gaussian basis sets, whose compactness is an important advantage in many-body calculations, as we have recently demonstrated (Pub. 8). Our open source PySCF project now provides start-of-the-art implementations of many molecular methods, competitive with the leading commercial quantum chemistry software packages. Our recent work has extended the base infrastructure (basis sets, integrals, mean-field solvers, and integral transformations) to periodic boundary conditions and Brillouin sampling. A unique feature of PySCF is that it provides this leading performance while being implemented primarily in Python, which greatly enhances ease-of-use.

II. PERSONNEL

Supported over the 3 year period.

- (postdoc) Barbara Sandhoefer (partial)
- (postdoc) Qiming Sun (partial)
- (postdoc) Alexander Sokolov (partial)
- (grad student) James McClain (partial)

III. BUDGET

- Projected remainder: 0K

[1] J. LeBlanc, A. E. Antipov, F. Becca, I. W. Bulik, G. K.-L. Chan, C.-M. Chung, Y. Deng, M. Ferrero, T. M. Henderson, C. A. Jiménez-Hoyos, et al., *Physical Review X* **5**, 041041 (2015).

[2] B.-X. Zheng, J. S. Kretchmer, H. Shi, S. Zhang, and G. K. Chan, *arXiv preprint arXiv:1608.03316* (2016).

[3] I. W. Bulik, G. E. Scuseria, and J. Dukelsky, *Physical Review B* **89**, 035140 (2014).

[4] I. W. Bulik, W. Chen, and G. E. Scuseria, *The Journal of chemical physics* **141**, 054113 (2014).

[5] M. Welborn, T. Tsuchimochi, and T. Van Voorhis, *The Journal of Chemical Physics* **145**, 074102 (2016).

[6] J. Qin, Q. Jie, and Z. Fan, *Computer Physics Communications* **204**, 38 (2016).

[7] B.-X. Zheng and G. K.-L. Chan, *Physical Review B* **93**, 035126 (2016).

[8] J. Yang, W. Hu, D. Usvyat, D. M. and M. Schuetz, and G. K.-L. Chan, *Science* **345**, 640 (2014).

[9] J. McClain, J. Lischner, T. Watson, D. A. Matthews, E. Ronca, S. G. Louie, T. C. Berkelbach, and G. K.-L. Chan, *Phys. Rev. B* **93**, 235139 (2016).